Electronic Supplementary Material (ESI) for Nanoscale.
This journal is © The Royal Society of Chemistry 2018

Supporting Information

Self-sensitization induced upconversion of Er^{3+} in core-shell nanoparticles

Long Yan,[a] Bo Zhou,[a,*] Nan Song,[a] Xuelong Liu,[a] Jinshu Huang,[a] Ting Wang,[a] Lili Tao,[b,*] and Qinyuan Zhang[a,*]

[a] *State Key Laboratory of Luminescent Materials and Devices, Guangdong Provincial Key Laboratory of Fiber Laser Materials and Applied Techniques, and Institute of Optical Communication Materials, South China University of Technology, Guangzhou, 510641, China.*

[b] *School of Materials and Energy, Guangdong University of Technology, Guangzhou, 510006, China.*

E-mails: (B.Z.) zhoubo@scut.edu.cn; (L.T.) taoll@gdut.edu.cn; (Q.Z.) qyzhang@scut.edu.cn

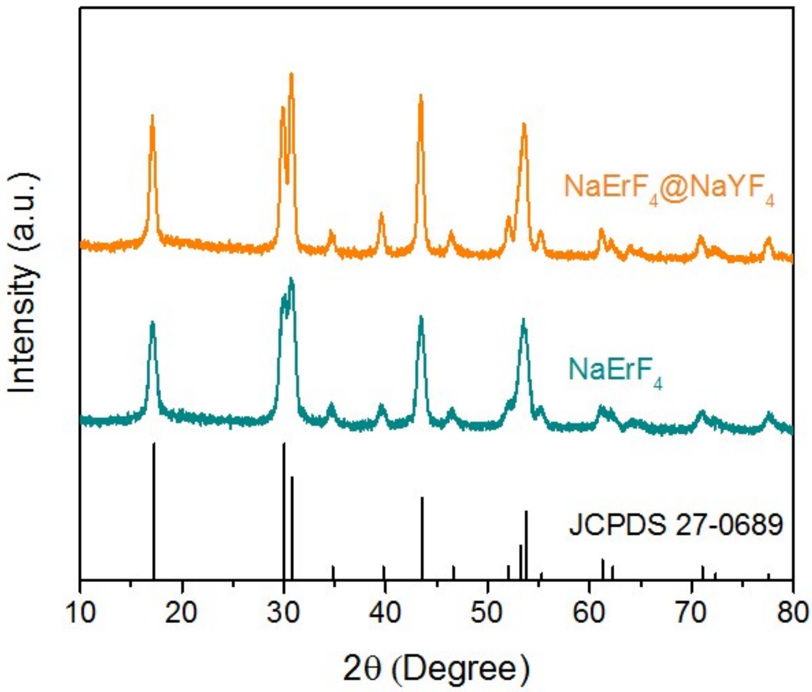

Figure S1. XRD patterns of $NaErF_4$ core and $NaErF_4$@$NaYF_4$ core-shell nanoparticles. Note that their morphology is shown in TEM images of Fig 2a,b in maintext. The card JCPDS 27-0689 is from hexagonal phase $NaErF_4$.

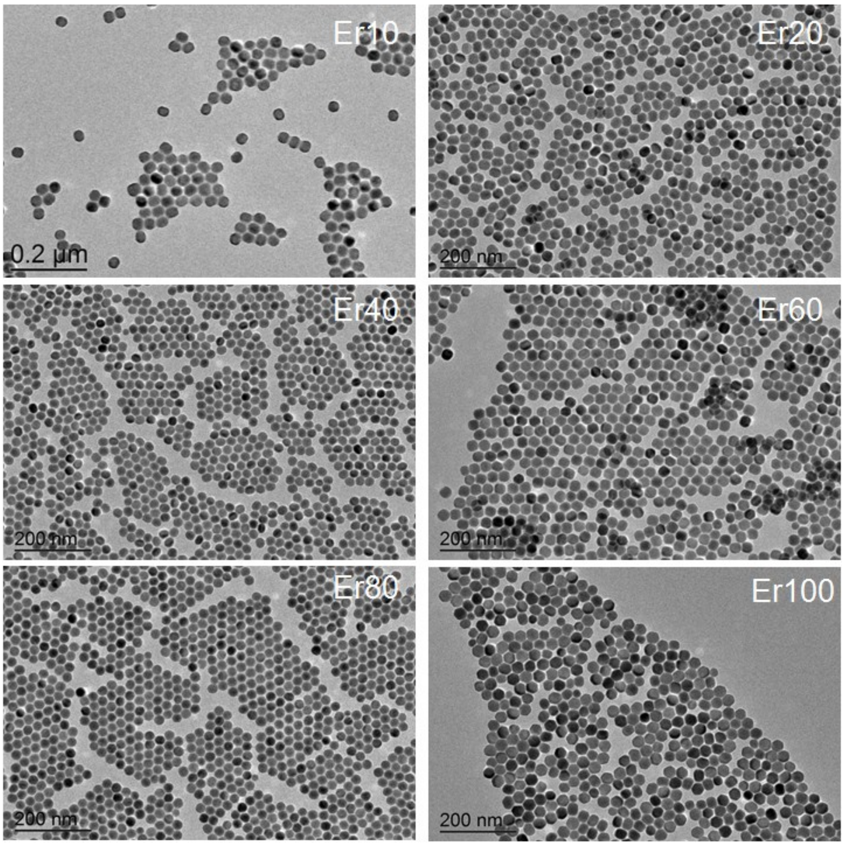

Figure S2. TEM images of as-prepared $NaYF_4$:Er(1~100 mol%) nanoparticles showing no obvious change on the morphology with increasing Er^{3+} concentration. The marks Er10, Er20, Er40, Er60, Er80 and Er100 stand for the dopant concentration of 10, 20, 40, 60, 80 and 100 mol%, respectively.

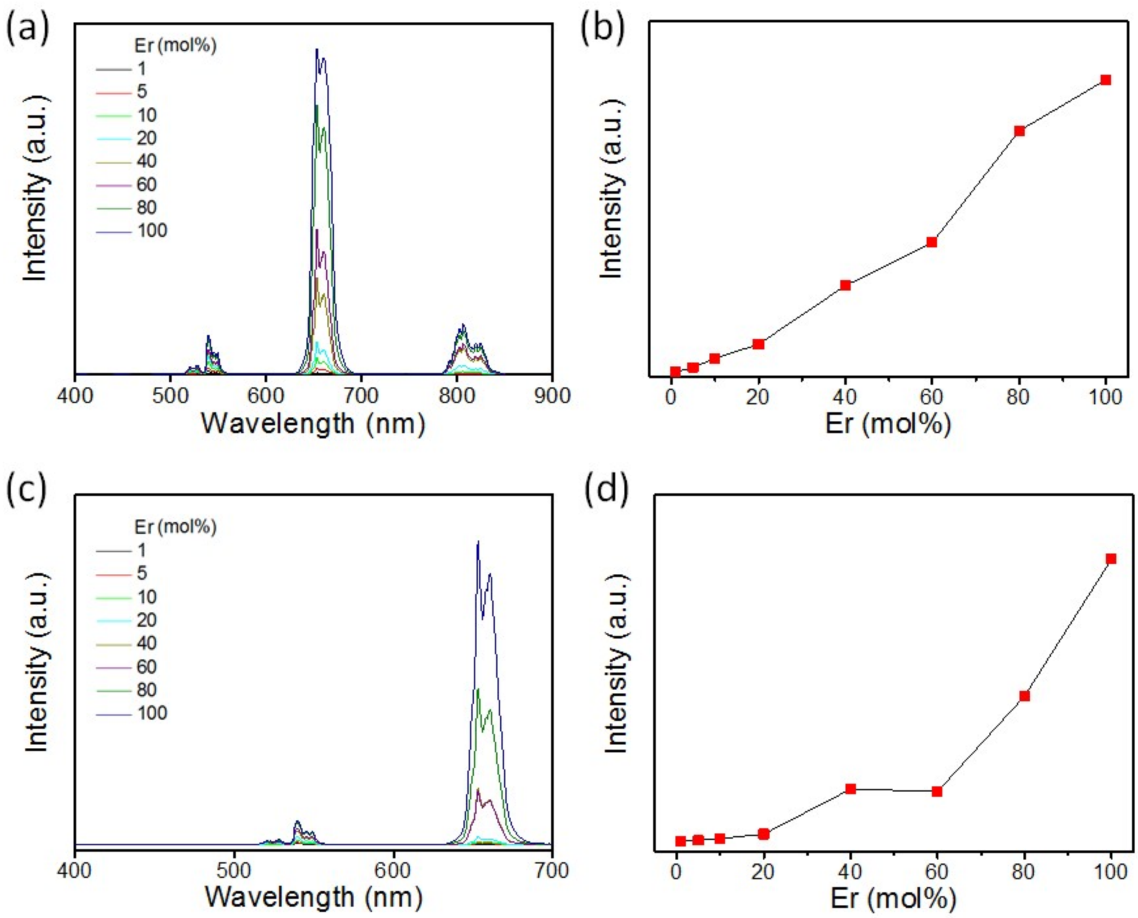

Figure S3. (a,c) Upconversion emission spectra of $NaYF_4$:Er(1~100 mol%)@$NaYF_4$ core-shell nanoparticles under (a) 980 nm and (c) 808 nm excitations. (b,d) The dependence of red upconversion emission intensity on the Er^{3+} dopant concentration in core for (a,c) samples under (a) 980 nm and (c) 808 nm excitations, respectively.

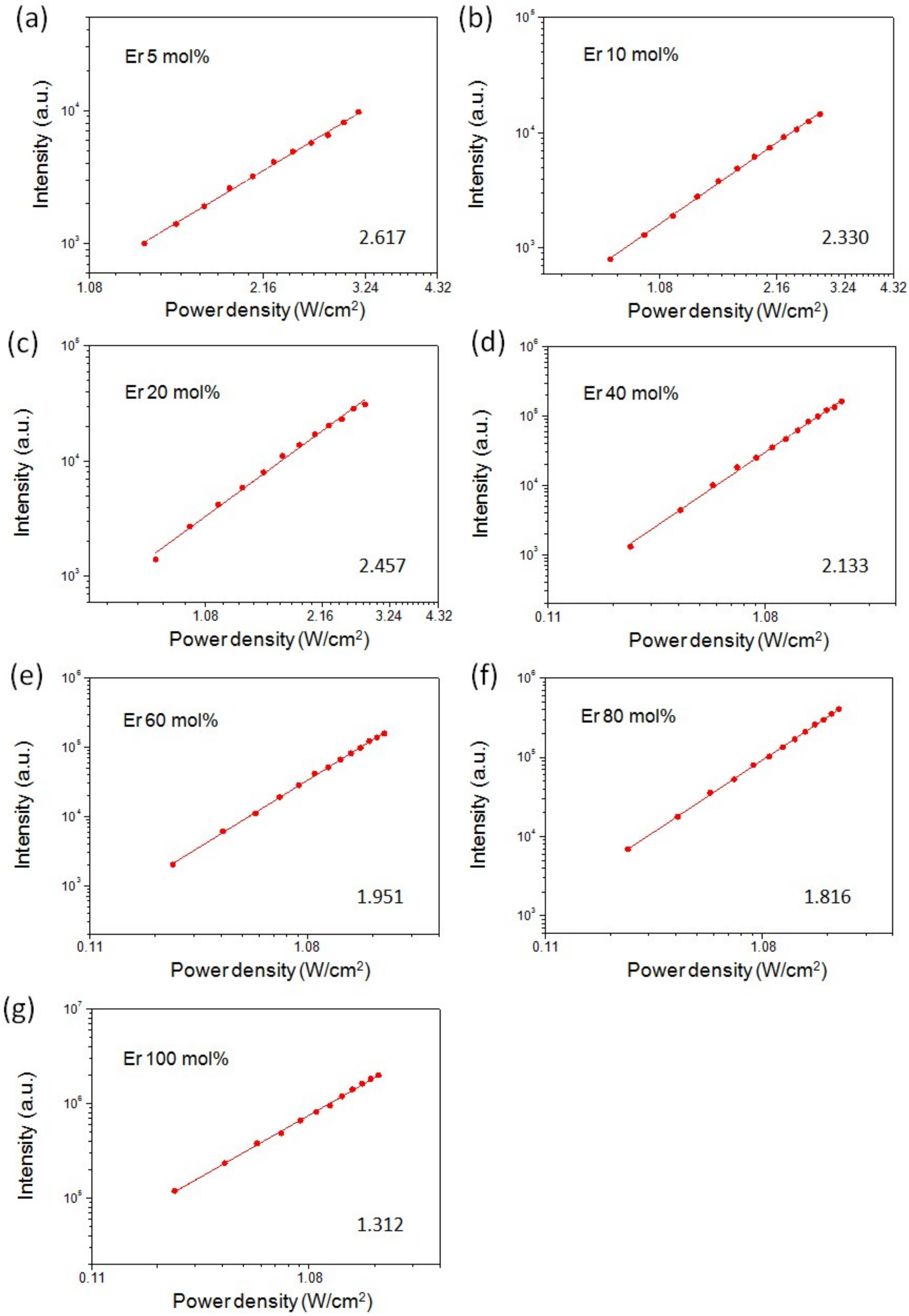

Figure S4. Dependence of the red upconversion emission intensity on the pump power density for $NaYF_4$:Er(5~100 mol%)@$NaYF_4$ core-shell nanoparticles with Er^{3+} dopant concentration under the 1530 nm excitation. The fitted slope values are plotted in each panels.

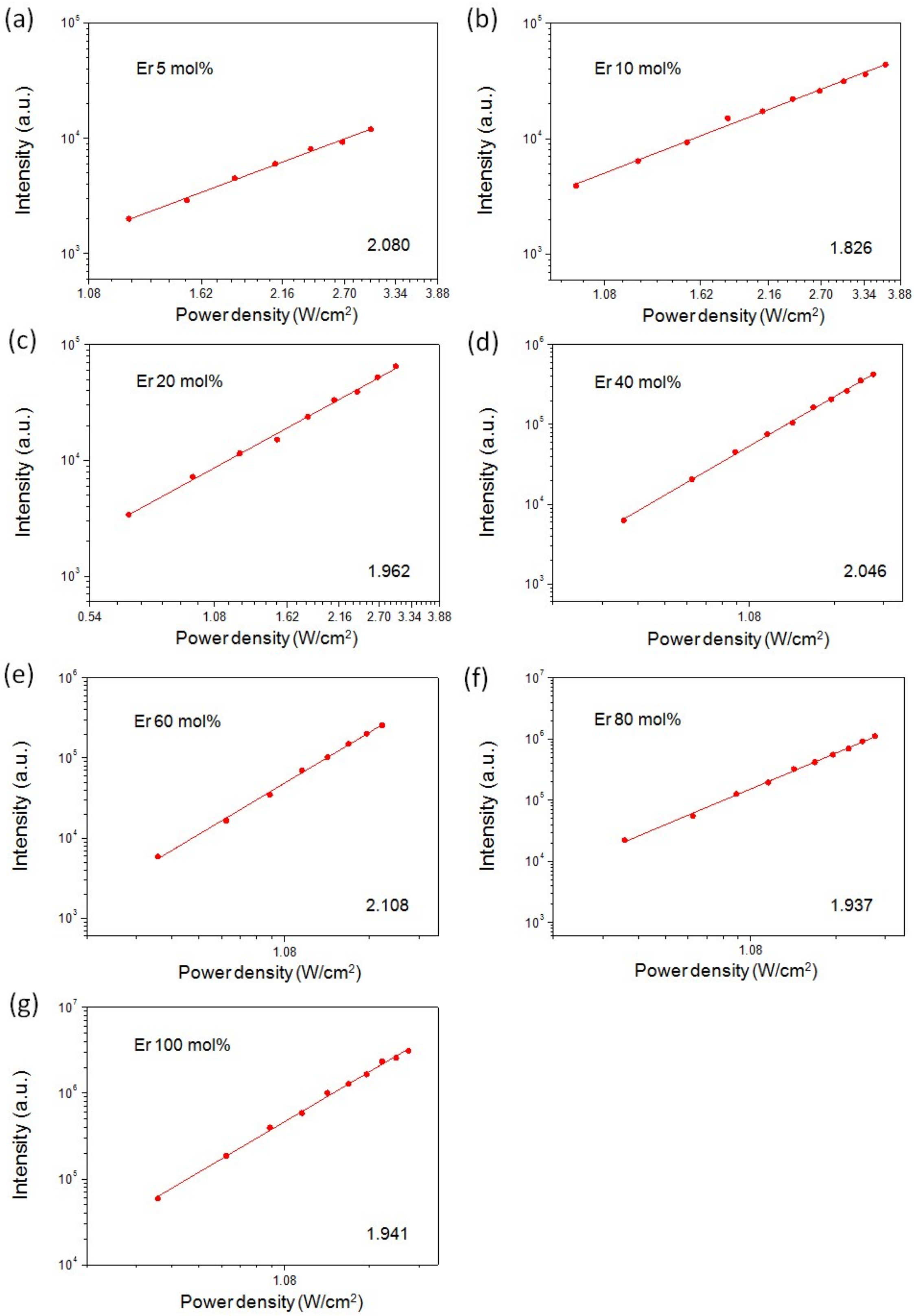

Figure S5. Dependence of the red upconversion emission intensity on the pump power density for $NaYF_4$:Er(5~100 mol%)@$NaYF_4$ core-shell nanoparticles with Er^{3+} dopant concentration under the 980 nm excitation. The fitted slope values are plotted in each panels.

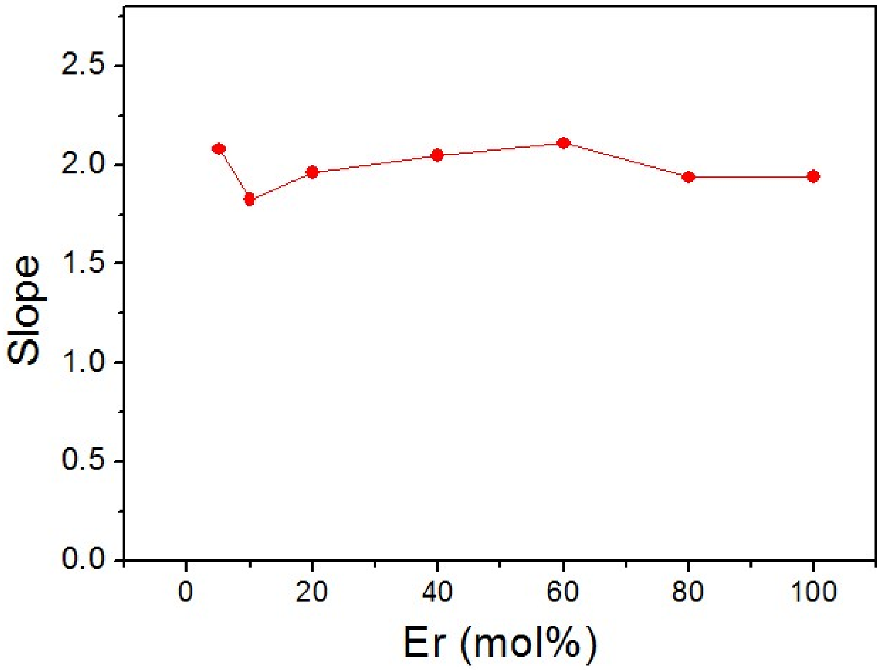

Figure S6. Dependence of the fitted slope values for the red upconversion emission intensity on the Er^{3+} dopant concentration in $NaYF_4$:Er(5~100 mol%)@$NaYF_4$ under the 980 nm excitation.

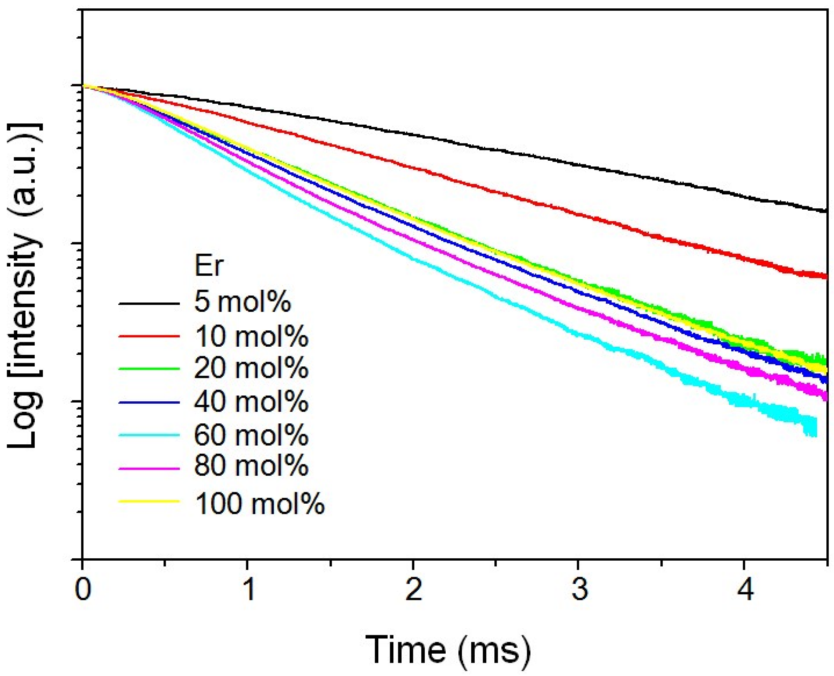

Figure S7. Decay curves of Er^{3+} at its $^4F_{9/2}$ state from $NaYF_4$:Er@$NaYF_4$ core-shell nanoparticles under pulsed 1530 nm excitation.

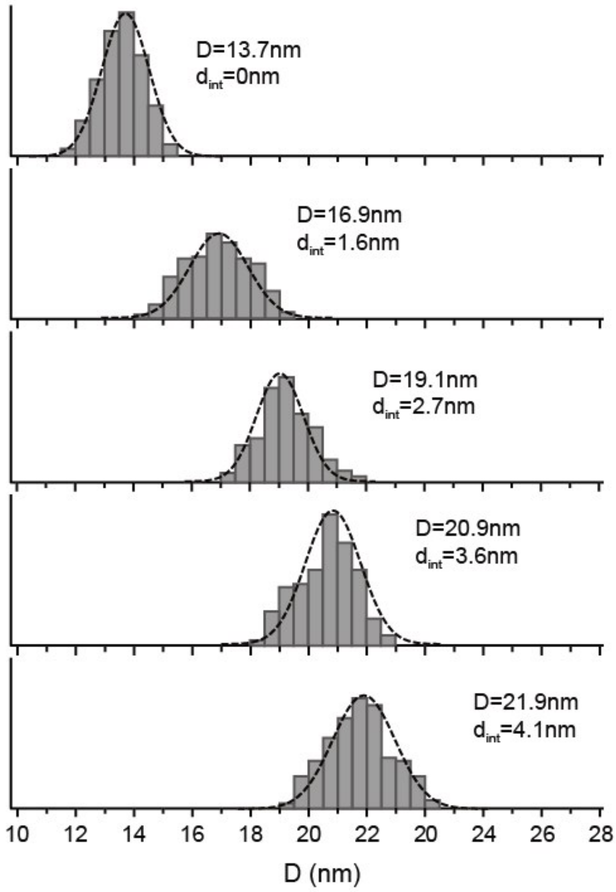

Figure S8. The size distribution of the nanoparticles in Fig. 5a in the maintext. Note that D and d_{int} stand for diameter and interlayer thickness, respectively.

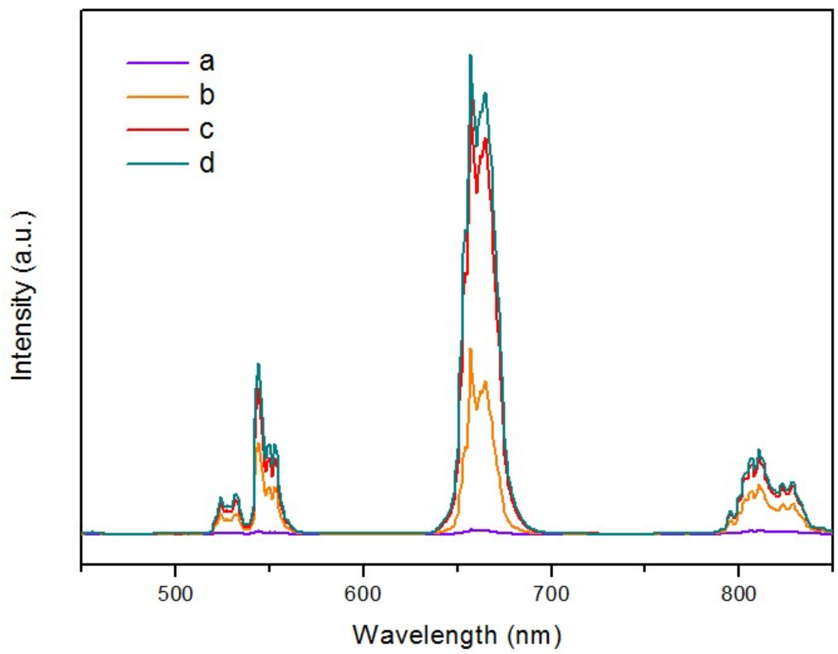

Figure S9. Upconversion emission spectra of $NaErF_4$@$NaYF_4$ core-shell nanoparticles with the $NaYF_4$ shell thickness of (a) 1.6 nm, (b) 2.7 nm, (c) 3.6 nm and (d) 4.1 nm.

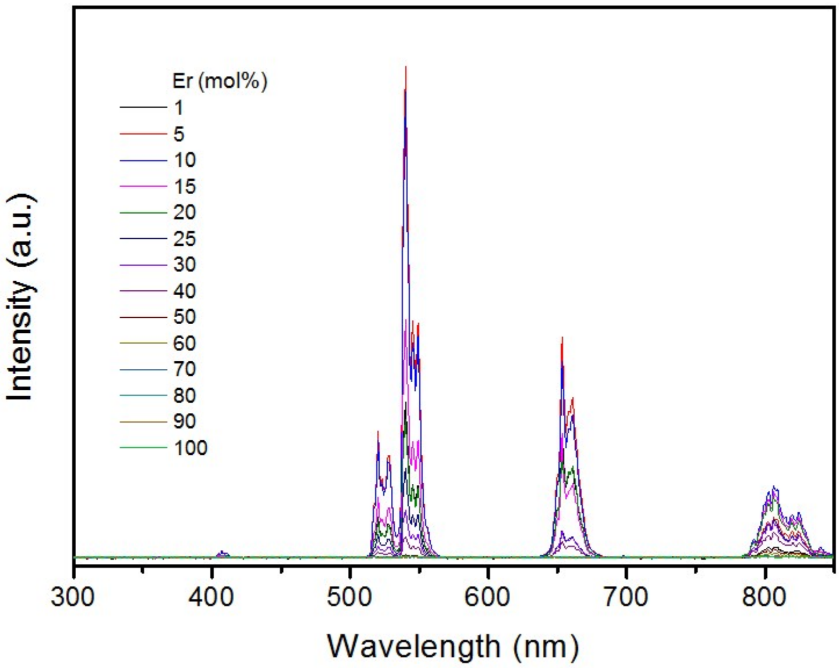

Figure S10. Upconversion emission spectra of $NaYF_4$:Er(1~100 mol%) core only nanoparticles under 1530 nm excitation.

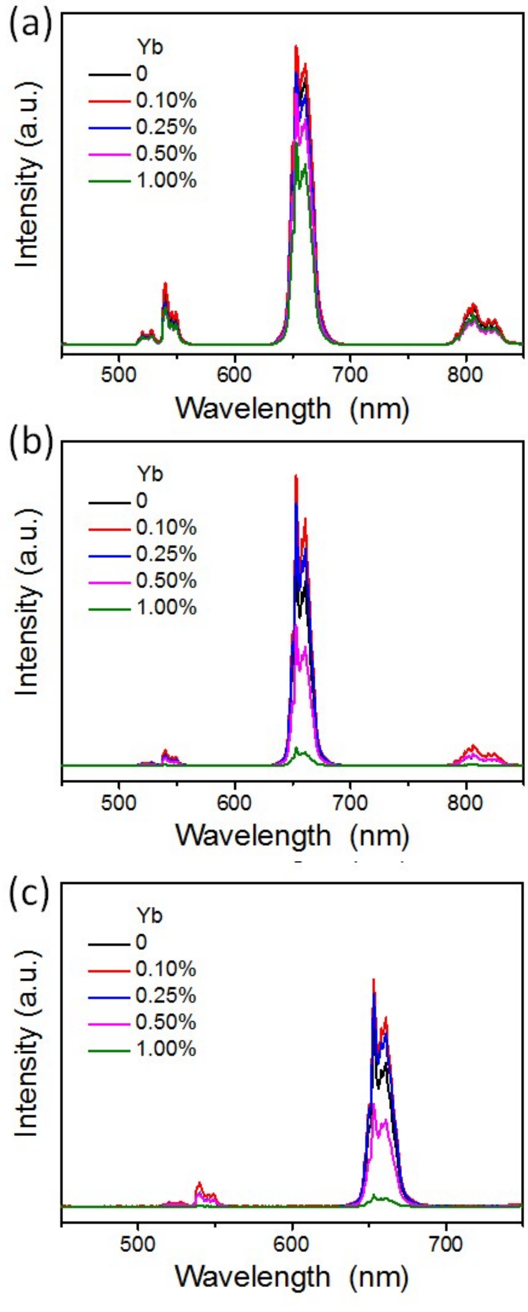

Figure S11. Upconversion emission spectra of $NaErF_4$:Yb(0~1 mol%)@$NaYF_4$ core-shell samples under (a) 1530 nm, (b) 980 nm and (c) 808 nm excitations.

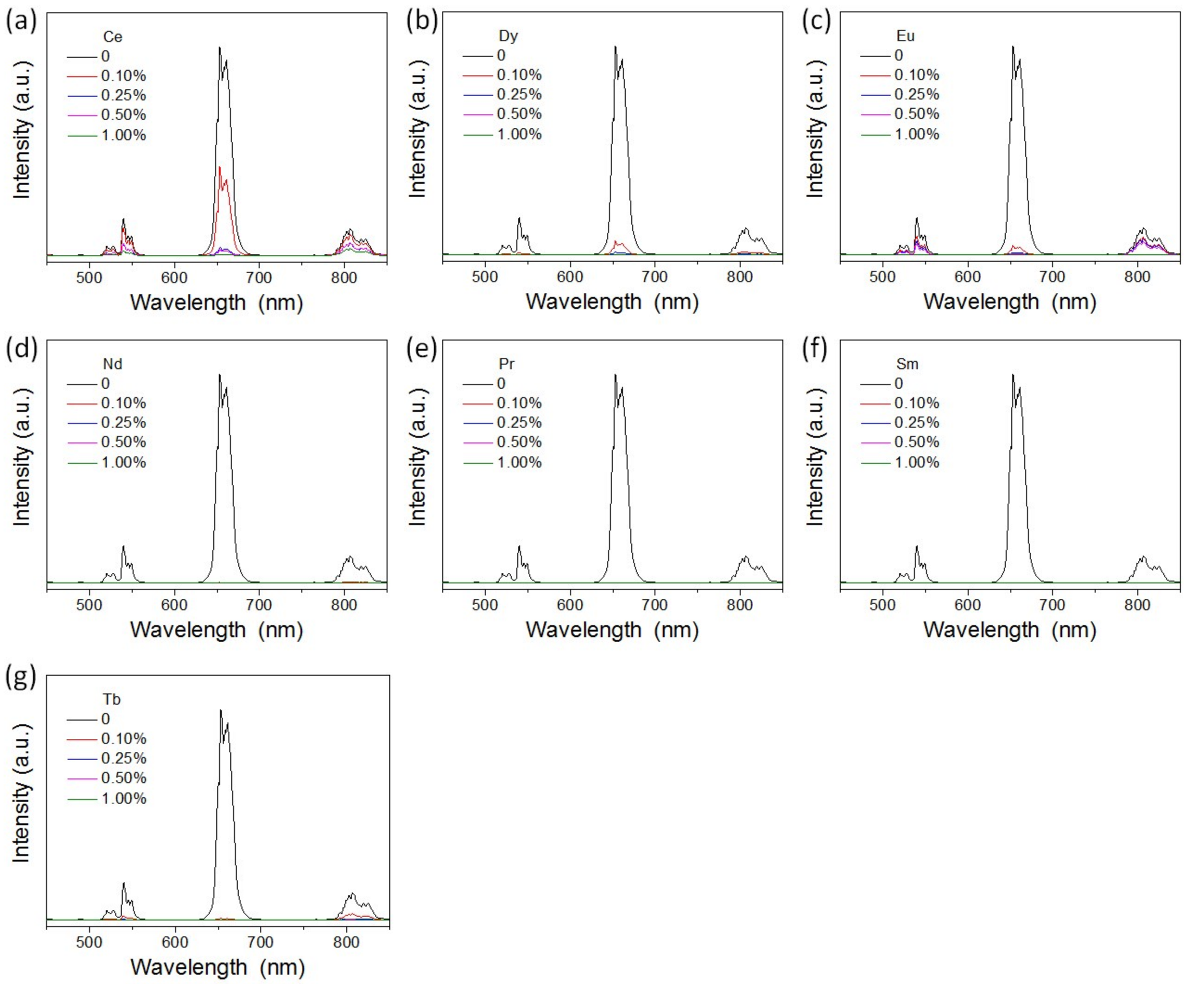

Figure S12. Upconversion emission spectra of $NaErF_4$:Ln(0~1 mol%)@$NaYF_4$ core-shell samples under 1530 nm excitation for dopants of (a) Ce^{3+}, (b) Dy^{3+}, (c) Eu^{3+}, (d) Nd^{3+}, (e) Pr^{3+}, (f) Sm^{3+}, and (g) Tb^{3+}.

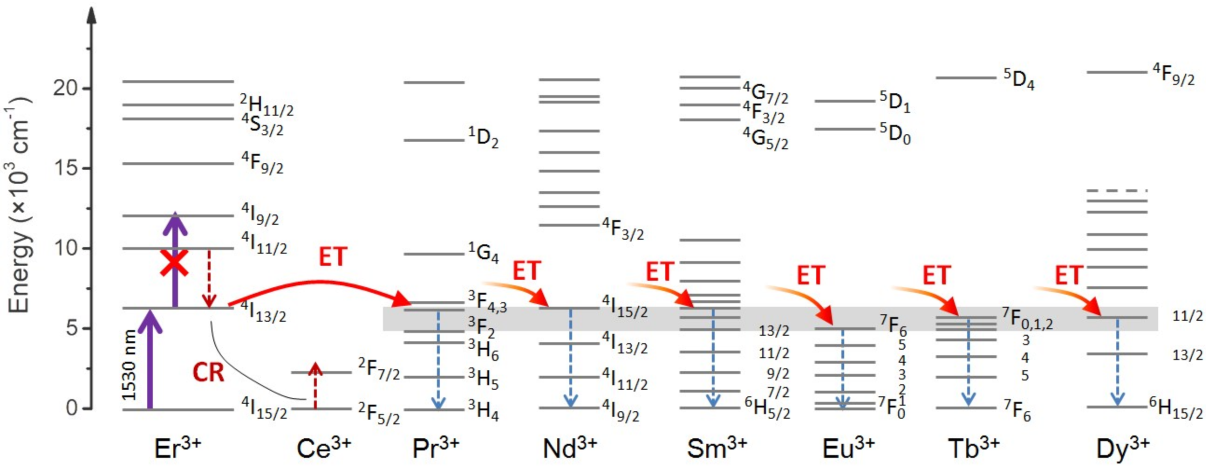

Figure S13. Schematic illustration of possible energy transfer (ET) and cross relaxation (CR) processes occuring Er^{3+} and other lanthanides (Ce^{3+}, Pr^{3+}, Nd^{3+}, Sm^{3+}, Eu^{3+}, Tb^{3+} and Dy^{3+}) that may lead to a quenching of upconversion through depopulating the Er^{3+} ($^4I_{13/2}$) level. Note that cross relaxation process may also occur for Pr^{3+}, Nd^{3+}, Sm^{3+}, Eu^{3+}, Tb^{3+} and Dy^{3+} due to the energy matching for the relevant transitions.

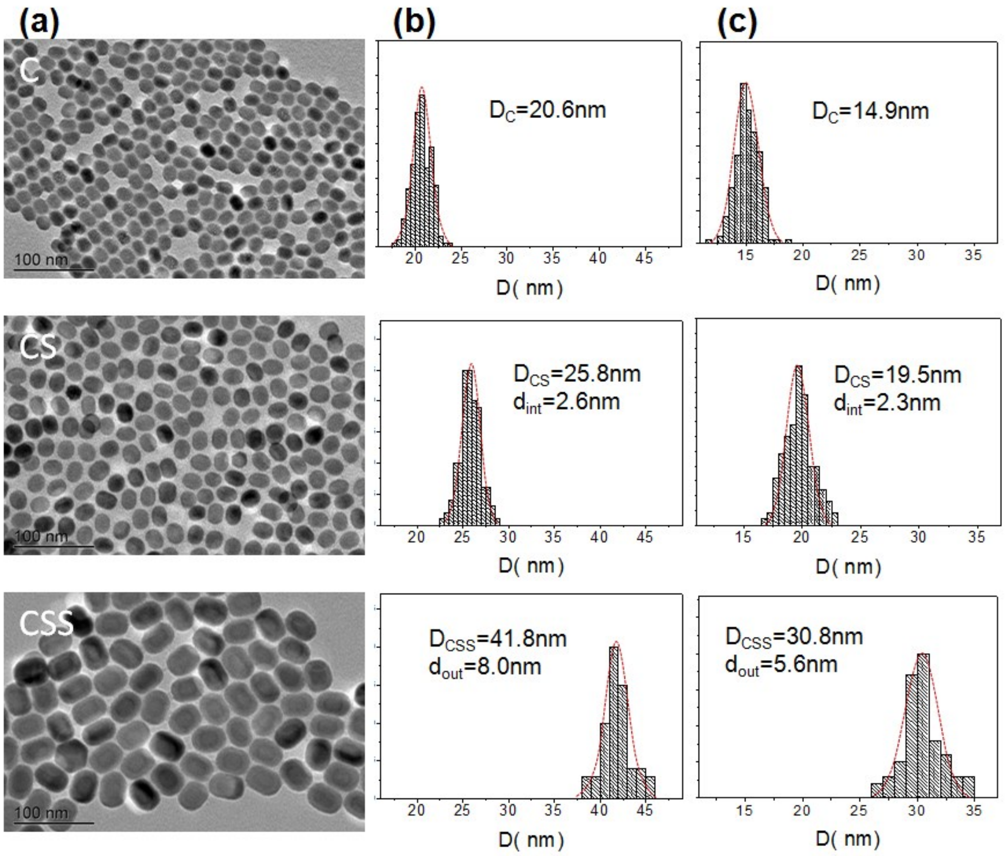

Figure S14. (a) TEM images of $NaYF_4$ core (C), $NaYF_4$@$NaErF_4$ core-shell (CS) and $NaYF_4$@$NaErF_4$@$NaYF_4$ core-shell-shell (CSS) nanoparticels. (b,c) The size distribution of the (a) nanoparticles at the major axis (b) and the minor axis (c) directions. The interlayer and the outer shell layer thicknesses are also presented. Note that D, d_{int} and d_{out} stand for diameter, interlayer and outer shell thickness, respectively.

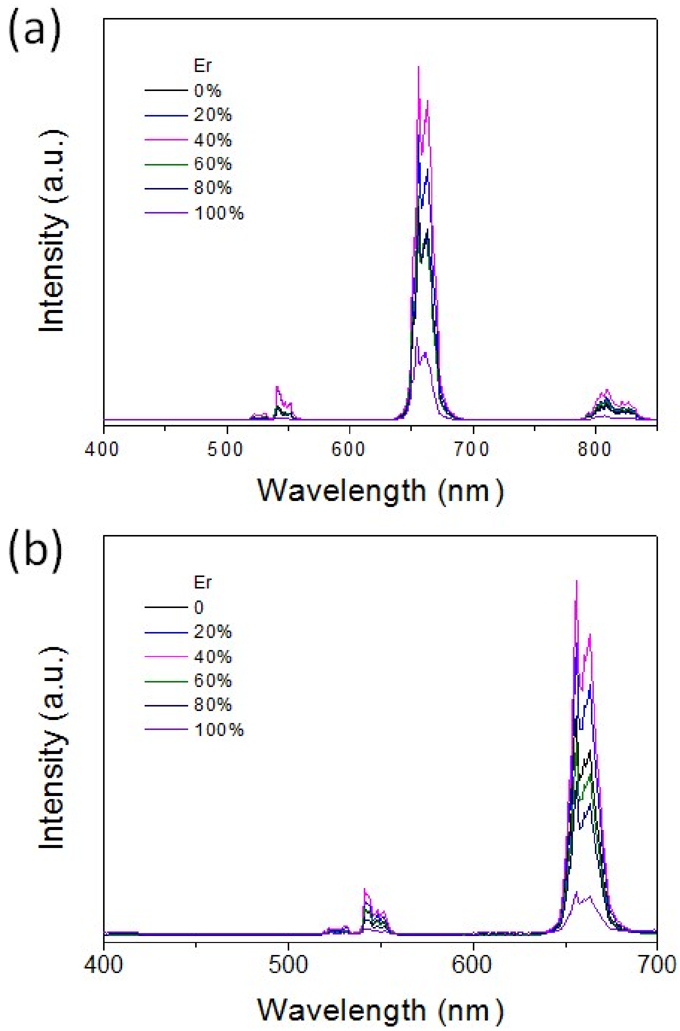

Figure S15. Upconversion emission spectra of $NaYF_4$:Er(0~100 mol%)@$NaErF_4$@$NaYF_4$ core-shell-shell samples under (a) 980 nm and (b) 808 nm excitations.